THE JOURNAL OF PHYSICAL CHEMISTRY Letters

Letter

pubs.acs.org/JPCL

Measurement of the Hydrophobic Force in a Soft Matter System

Rico F. Tabor,*[,†] Chu Wu,[‡,§] Franz Grieser,[‡,∥] Raymond R. Dagastine,[‡,⊥,#] and Derek Y. C. Chan*[,‡,§,▽]

[†]School of Chemistry, Monash University, Clayton 3800, Australia

[‡]Particulate Fluids Processing Centre, University of Melbourne, Parkville 3010, Australia

[§]Department of Mathematics and Statistics, University of Melbourne, Parkville 3010, Australia

[∥]School of Chemistry, University of Melbourne, Parkville 3010, Australia

[⊥]Department of Chemical and Biomolecular Engineering, University of Melbourne, Parkville 3010, Australia

[#]Melbourne Centre for Nanofabrication, 151 Wellington Road, Clayton, Victoria, 3168, Australia

[▽]Faculty of Life and Social Sciences, Swinburne University of Technology, Hawthorn 3122, Australia

Web-Enhanced Feature *Supporting Information*

ABSTRACT: The hydrophobic attraction describes the well-known tendency for nonpolar molecules and surfaces to agglomerate in water, controlled by the reorganization of intervening water molecules to minimize disruption to their hydrogen bonding network. Measurements of the attraction between chemically hydrophobised solid surfaces have reported ranges varying from tens to hundreds of nanometers, all attributed to hydrophobic forces. Here, by studying the interaction between two hydrophobic oil drops in water under well-controlled conditions where all known surface forces are suppressed, we observe only a strong, short-ranged attraction with an exponential decay length of 0.30 ± 0.03 nm—comparable to molecular correlations of water molecules. This attraction is implicated in a range of fundamental phenomena from self-assembled monolayer formation to the action of membrane proteins and nonstick surface coatings.

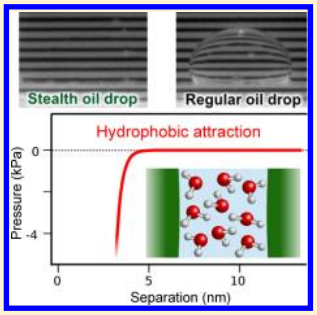

SECTION: Glasses, Colloids, Polymers, and Soft Matter

The hydrophobic effect underpins familiar observations such as the separation of salad dressing[1] or the difficulty of dispersing oil spills. It also has fundamental implications for living organisms in determining polypeptide conformation and cellular membrane assembly.[2,3] The underlying chemistry, characterized by the high entropic component of the unfavorable solvation free energy of nonpolar solutes, is attributed to water molecules rearranging themselves around such moieties in order to maximize opportunities for hydrogen bonding.[3] How such an effect is manifested in the interaction between supramolecular to mesoscopic surfaces, of relevance for instance, to surface engineering using self-assembled monolayers, has driven an ongoing quest to quantify its range and intensity.[4−6]

Ever since the first experiments were conducted some 30−40 years ago,[3,7] direct measurements of the hydrophobic interaction between surfaces have largely been made by coating smooth mica or silica substrates with organic molecular layers, deposited by adsorption or chemical bonding from water or organic solvents. The term 'hydrophobic interaction' describes observations that deviate from the expected electrical double layer repulsion and van der Waals attraction under the Derjaguin−Landau−Verwey−Overbeek (DLVO) model of surface forces.[8] With a broad reported range from a few nanometers up to an astonishing 650 nm,[9] the experimental situation has continued to remain "murkier rather than clearer[6]". The additional attraction has been attributed to arise from adsorbed mobile molecular layers rearranging to form charged patches on the surfaces.[4,10] Further subtleties arise if species within the hydrophobic layer can change conformation during interaction.[11] Capillary bridging by nanobubbles formed on hydrophobic surfaces provides another source of strong, long-range attraction:[12−14] degassing the water affects the range and magnitude.[13] Therefore where solid surfaces have been rendered hydrophobic by surface modification, different mechanisms, perhaps not directly related to the molecular properties of water, seem to be responsible for the additional attraction between such hydrophobised solid surfaces.

On the other hand, long-range hydrophobic interactions have never been observed in force measurements between soft hydrophobic systems such as oil drops and gas bubbles.[15,16] This disconnect suggests that the long-range forces seen between hydrophobised solid surfaces are not directly specific to hydrophobes *per se*, but nonetheless must be recognized in addition to any intrinsic hydrophobic interaction that originates from water structuring around extended nonpolar surfaces.[5]

Here, by completely suppressing the contribution from all known forces between two well-characterized and inert oil droplets in water, we isolate and measure the residual attraction

Received: September 25, 2013
Accepted: October 31, 2013
Published: October 31, 2013

 © 2013 American Chemical Society dx.doi.org/10.1021/jz402068k | *J. Phys. Chem. Lett.* 2013, 4, 3872−3877

between such extended nonpolar surfaces by observing coalescence events over a broad range of dynamic conditions. Using a prescribed mixture of completely miscible perfluorooctane (PFO, C_8F_{18}) and perfluorobenzene (PFB, C_6F_6), liquids that have refractive indices below and above that of water, we create a mixture (PFX) that is refractive index-matched to water. This minimizes, as far as practicable, the van der Waals (vdW) attraction between such drops in water[8]—a condition that has not been exploited before in the context of direct force measurements. By operating close to the isoelectric point of PFX (pH 3.0)[17] and under high salt concentrations, we also suppress the electrical double layer (EDL) interaction. The extent to which vdW and EDL interactions can be controlled is demonstrated in Figure 1A and a visual demonstration of the

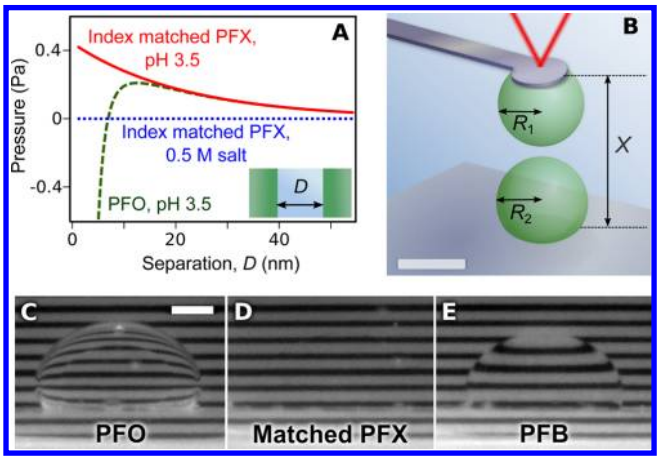

Figure 1. Perfluorooctane (PFO), perfluorobenzene (PFB), and refractive index matched mixture (PFX) drops in water. (A) Calculated disjoining pressure due to electrical double layer repulsion (EDL) and van der Waals (vdW) attraction between two half spaces (see Inset) of fluorocarbon-oils across electrolyte: PFO with surface potential 16 mV at a solution pH 3.5 and no added salt (green, dashed line) showing EDL repulsion at large separations and vdW attraction at small separations; PFX drops with surface potential 16 mV at a solution pH 3.5 and no added salt (red, solid line) with EDL repulsion but vdW attraction suppressed; PFX drops in 0.5 M salt (dotted, blue line) with both EDL repulsion and vdW attraction suppressed. See Supporting Information for details. (B) A schematic representation of the force measurement experiment between two drops in the atomic force microscope in the axisymmetric configuration. The scale bar represents 100 μm. (C) Photograph of a PFO sessile drop with refractive index 1.26. The scale bar represents 1 mm; (D) a PFX sessile drop with refractive index 1.33, matched to water; and (E) a PFB sessile drop with refractive index 1.37.

degree of refractive index-matching is shown in Figure 1C−E. The fluorocarbons are over 5 times less water-soluble than their hydrocarbon counterparts, so their interface with water is molecularly smooth without the self-organized features that might occur on solid substrates with adsorbed amphiphiles. The three interfacial tensions involving PFX, water and air cannot satisfy the Neumann triangle condition, so nanobubbles cannot be sustained at the fluorocarbon−water interface.[18] Therefore we have, as far as possible, eliminated all known interactions in such a system of 'stealth' PFX drops in water and suppressed mechanisms that might be responsible for the observed long-ranged attractions between hydrophobised solid surfaces.

We study the coalescence of two oil drops in aqueous electrolyte in axisymmetric alignment, using an atomic force microscope[19] (AFM, Figure 1B). The drops are driven toward and then away from each other by varying the separation, $X(t)$, between the cantilever and the substrate. The drive speeds range from a quasi-equilibrium value of 0.1 μm/s to 25 μm/s, well above Brownian velocities where hydrodynamic interactions and surface deformations are important. The maximum displacement is set to ensure that the drops will interact and deform. In some cases, depending on the velocity and maximum displacement, the two drops remain distinct when separated. In others, the drops coalesce − either while being driven together or when they are being separated. The measured time variation of the interaction force and the time of drop coalescence under different drive conditions is used to deduce the range and magnitude of the attraction between such 'stealth' drops for which all known surface interactions—namely, electrical double layer (EDL) and van der Waals (vdW) forces—have been suppressed as far as practicable (see Supporting Information for full experimental details).

First we demonstrate how the electrical double layer (EDL) force of electrostatic origin (Figure 2A), the van der Waals (vdW) force of quantum electrodynamic origin (Figure 2B), and the classical hydrodynamic force (Figure 2C) can be selected individually to provide the sole repulsive interaction between different types of oil drops in aqueous electrolyte as they are pushed together to the very moment the hydrophobic attraction triggers coalescence.

By working at pH 3.5 with no added salt, only the EDL repulsion operates between two PFX drops because the vdW interaction is minimized in such drops that are index-matched with water (Figure 2A). In contrast, by using different oils and working in 1 M $NaNO_3$ electrolyte, we have only the vdW repulsion between a pure PFO drop (refractive index 1.26) and a pure tetradecane drop (TD, $C_{14}H_{30}$, refractive index 1.43) as the EDL interaction is screened by the high salt concentration (Figure 2B). In both cases, the drops are brought together at a quasi-equilibrium speed of 0.1 μm/s (negligible hydrodynamic force), therefore drop coalescence (indicated by solid arrows) is triggered by the only remaining force, namely, hydrophobic attraction, after reaching a force maximum of the order of 1 nN.

The use of the hydrodynamic repulsion between two PFX drops to probe the hydrophobic attraction is shown in Figure 2C. The drops are driven together at 20 μm/s in 1 M $NaClO_4$ so both vdW and EDL interactions are now suppressed. The hydrophobic attraction induced coalescence occurs at a force that is around 50 times higher than under quasi-equilibrium conditions (Figure 2A,B) because of strong hydrodynamic repulsion at a speed around 3 times the Brownian velocity of the drops.

To analyze the results in Figure 2 using a well-established theory of interactions between deformable drops,[15,20,21] accurately quantified estimates of vdW, EDL and hydrodynamic forces must be augmented with a model for the hydrophobic attraction.

The free energy per unit area of two planar half-spaces of oil separated by a film of water, thickness D, (Figure 1A) can be written generally as $G(D) = 2\gamma + E(D)$, where γ is the oil−water interfacial energy and $E(D)$ is the separation dependent interaction free energy. From thermodynamic considerations, it must have the limiting forms: (a) $E(D \to \infty) \to 0$, since the interaction must vanish when the surfaces are far apart, and (b) $E(D \to 0) \to -2\gamma$, because this is the zero-energy reference state of a bulk oil material without an interface. In a stealth system, only the hydrophobic interaction contributes to γ. The interfacial energy of the PFX−water system is $\gamma \approx 50$ mJ/m^2

dx.doi.org/10.1021/jz402068k | J. Phys. Chem. Lett. 2013, 4, 3872−3877

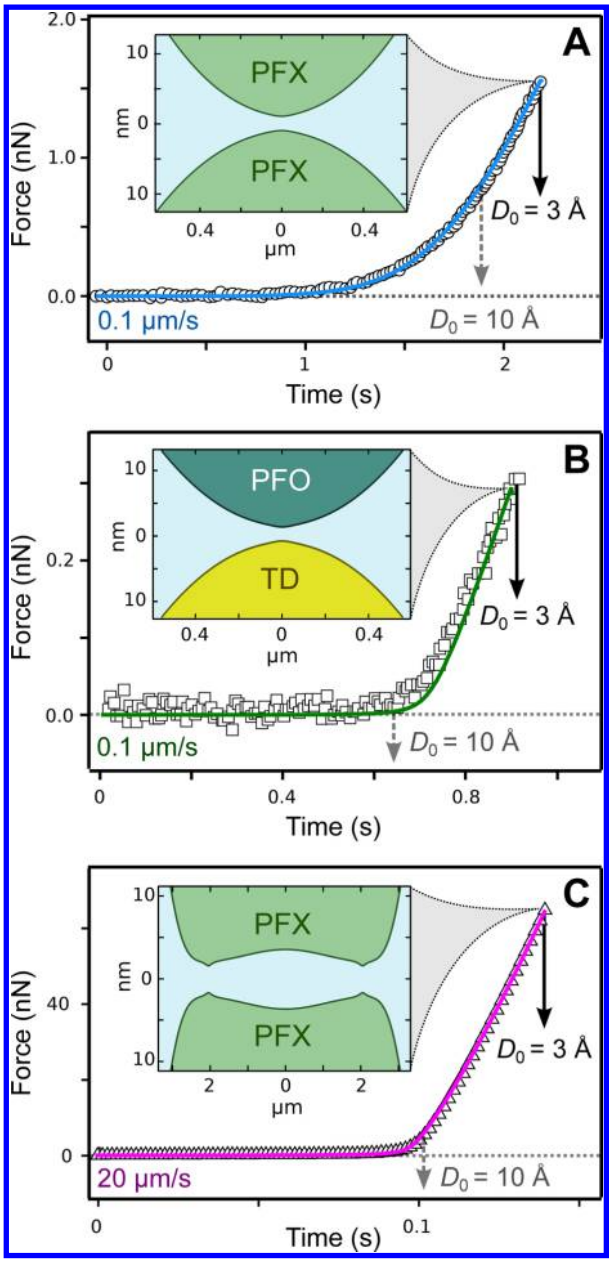

Figure 2. Force between oil drops in aqueous electrolyte approaching at various speeds prior to coalescence. Measured (hollow symbols) and calculated (line) forces are shown as functions of time. Scatter in the data points is indicative of the experimental tolerance. Prior to coalescence triggered by short-ranged hydrophobic attraction (down arrows), the force is due to (A) electrical double layer repulsion between PFX (index-matched) drops at pH 3.5 with no added salt (radii 43 and 40 μm) approaching at 0.1 μm/s; (B) van der Waals repulsion between a PFO and a tetradecane drop at pH 3.5 and 1 M $NaNO_3$ (radii 39 and 41 μm) approaching at 0.1 μm/s; (C) hydrodynamic repulsion between two (index-matched) PFX drops in 1 M $NaClO_4$ (radii 31 and 34 μm) approaching at 20 μm/s. Down arrows indicate coalescence point predicted with eq 1 using a decay length (D_0) of 0.30 nm (solid arrows) or 1.0 nm (dashed arrows). Insets: Calculated drop shapes and separation at the point of coalescence. For full experimental parameters, refer to Supporting Information.

(see Supporting Information). The Lum–Chandler–Weeks[22,23] theory of water structure at the air–water interface predicted an exponential correlation length of 0.38 nm. Extending this to the PBX–water system, we assume an exponential form for the hydrophobic interaction free energy per unit area, $E_{HB}(D)$, with a decay length D_o, that corresponds to the hydrophobic disjoining pressure:

$$\Pi_{HB}(D) = -\frac{dE_{HB}}{dD} = -\frac{2\gamma}{D_o}\exp(-D/D_o) \quad (1)$$

Predictions based on eq 1, shown as lines in Figure 2, for the three coalescence experiments taken over AFM drive speeds between 0.1 μm/s to 20 μm/s, all correspond to D_o = 0.30 ± 0.03 nm. Clearly with the more repulsive hydrodynamic interaction in Figure 2C, the experiment samples the more attractive region of the hydrophobic attraction in eq 1 that occurs at smaller separation. Thus by varying the magnitude of the hydrodynamic repulsion by controlling the AFM drive speed, different parts of the function $\Pi_{HB}(D)$ can be sampled. Such results are summarized in Figure 3 (see also Movie 1). If the decay length in eq 1 is increased to 1 nm, a value often reported as the hydrophobic decay length,[4−7] coalescence would occur too early and at a much lower force as indicated by the dashed arrows in Figures 2A–C. The drops shapes, calculated using the well-established theory for interactions between deformable drops (see Supporting Information for full

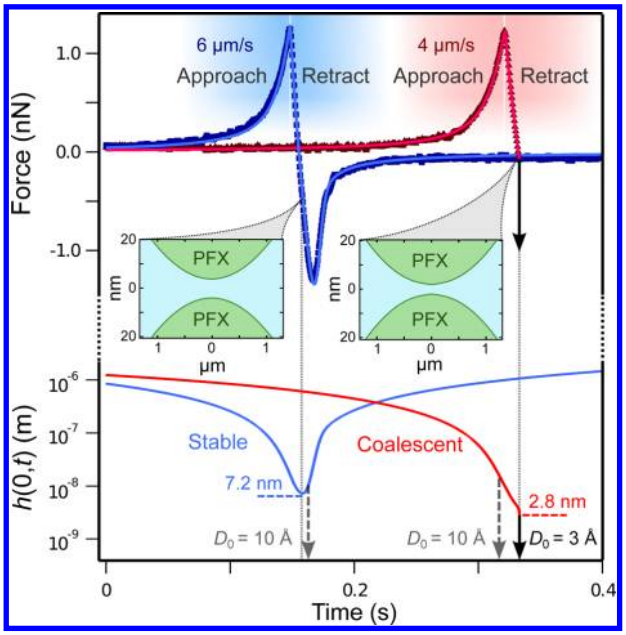

Figure 3. Results of dynamic measurements of the hydrophobic attraction using stealth drops. Two index-matched PFX drops under stealth conditions, in which electrical double layer and van der Waals forces are suppressed (1 M $NaClO_4$, radii 37 and 40 μm), are driven under two different approach-retract cycles. Time variations of the force, measured (filled symbols) and calculated using eq 1 (lines) are given with the calculated separation at the axis of symmetry, $h(0, t)$. At a drive velocity of 6 μm/s, the two drops separated on retraction after reaching a minimum separation of 7.2 nm (Stable, blue). At a drive velocity of 4 μm/s, the drops coalesced (down arrow) when they reached a minimum separation of 2.8 nm during the retraction cycle (Coalescent, red). Down arrows indicate coalescence point predicted with eq 1 using a 0.30 nm decay length (solid arrows) or a 1.0 nm decay length (dashed arrows). Inset: Calculated drop shapes and separation just before coalescence and for the stable case, at the minimum separation that occurred during the retraction phase but before the force minimum. For full experimental parameters, refer to the Supporting Information.

dx.doi.org/10.1021/jz402068k | J. Phys. Chem. Lett. 2013, 4, 3872–3877

details), just prior to coalescence are also shown as insets in Figure 2. In the quasi-equilibrium cases, insets to Figure 2A and 2B, the drops jump into contact when the separation at the center of symmetry reaches ~3 nm, whereas in the dynamic experiment at 20 μm/s (inset to Figure 2C), the drop surfaces are predicted to form a dimple and coalescence occurs when the separation at the dimple rim reaches ~3 nm (see Movie 2). The use of a power law for $\Pi_{HB}(D)$ does not provide agreement with experiments at all drive velocities (see Figure 4).

Thus, we see that for introduced repulsions between drops arising from three very different physical origins—electrostatic (EDL), quantum mechanical (vdW), and continuum hydrodynamics—in both quasi-equilibrium and dynamic measurements, the same short-range attractive force provides quantitative agreement with the force magnitude and the time at which coalescence occurs. This short-ranged hydrophobic attraction has a large magnitude dictated by thermodynamic considerations, and an exponential decay length of 0.30 ± 0.03 nm.

We also demonstrate that this short-ranged hydrophobic attraction can trigger the phenomenon of coalescence on separation.[24] After driving the drops together for some distance but before the drops coalesce, the cantilever on the AFM can be reversed to separate the drops. In Figure 3, results are shown for two index-matched PFX drops in 1 M $NaClO_4$ electrolyte, with both vdW and EDL interactions suppressed, subjected to two approach-retract cycles at slightly different velocities to impart different hydrodynamic interactions. Due to hydrodynamic suction, the minimum drop−drop separation is attained shortly after the commencement of the retraction phase.[16,25] It can be seen that when the retraction speed is not high enough, and this minimum separation falls to around 3 nm, the hydrophobic attraction triggers drop coalescence. Again, the hydrophobic disjoining pressure in eq 1 provides excellent agreement with the experimental results in Figure 3 (solid arrows). On the other hand, if the decay length of the hydrophobic attraction in eq 1 is increased to 1 nm, coalescence is predicted incorrectly for the stable case (6 μm/s), whereas for the 4 μm/s case coalescence is predicted to occur too early (dashed arrows).

In Figure 4A, we compare the measured force at the point of coalescence for 11 experiments with PFX drops with that predicted using the exponential form of the hydrophobic attraction with two different decay lengths: 0.30 and 1.0 nm, and with the power law with index n = 5 and 0.30 nm characteristic length (power law hydrophobic attraction: $\Pi_{HB}(D) = -(2n\gamma/D_o)\ [D_o/(D + D_o)]^{n+1}$; see Supporting Information). It is evident that representing the hydrophobic attraction by an exponential force law with a 0.30 ± 0.03 nm decay length provides consistent, quantitative agreement with the experimental data. An identical characteristic length was recently found experimentally for water near sapphire surfaces using a Brownian sampling technique, consistent with molecular dynamics modeling studies.[26]

We also summarize in Figure 4B the deduced drop separation at coalescence for 13 coalescence events during approach or retraction, at driving speeds of up to 25 μm/s and for PFX drops with mean radii between 25 and 50 μm. Electrolyte concentrations of 0.5 M $NaNO_3$, 1 M KI, or 1 M $NaClO_4$ were used to suppress the EDL repulsion. It is observed that the film thicknesses at coalescence cluster around 3 nm, as predicted by the hydrophobic attraction encapsulated

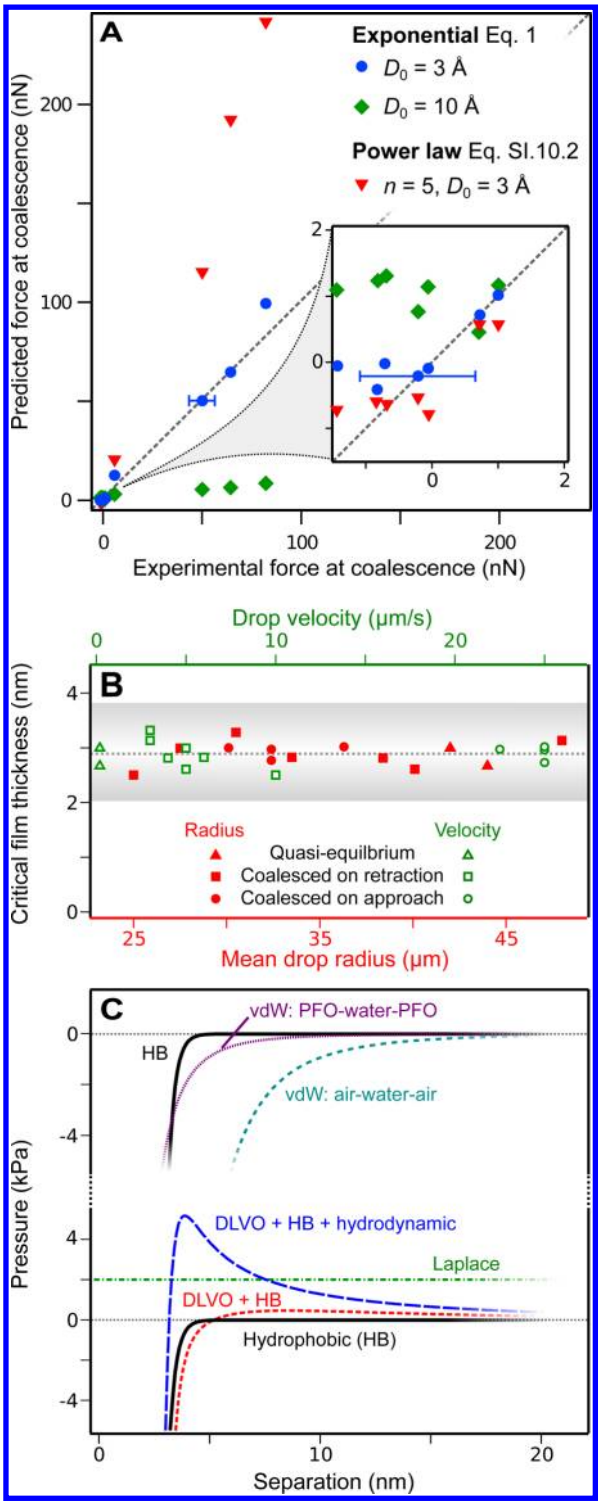

Figure 4. Force and film thickness at coalescence and comparison of disjoining pressures. (A) The measured force at coalescence between two index-matched PFX drops where only the hydrophobic attraction and hydrodynamic interaction operate compared to that predicted using three different forms for the hydrophobic attraction (filled symbols): the exponential law with 0.30 or 1.0 nm decay length or a power law[24] with power index n = 5 and characteristic length 0.30 nm given by eq 10.3 of the Supporting Information. Example error bars indicate the typical 95% confidence interval. (B) Compilation of the deduced film thickness directly prior to coalescence (filled and hollow symbols), from coalescence experiments between two index-matched PFX drops of mean drop radii: $R_h = (1/R_1 + 1/R_2)^{-1}$, at varying drive velocities. The electrolyte concentrations were 0.5 M $NaNO_3$ or 1 M

dx.doi.org/10.1021/jz402068k | J. Phys. Chem. Lett. 2013, 4, 3872−3877

Figure 4. continued

KI or 1 M $NaClO_4$. The gray band indicates the 95% confidence level. (**C**) Comparison of the magnitudes of the adopted exponential hydrophobic (HB) attractive pressure, (eq 1, D_o = 0.30 nm) with (upper pane) vdW attraction and (lower pane) the DLVO disjoining pressure for PFO drops at a surface potential of 10 mV at a solution pH 3.2 in 1 mM 1:1 electrolyte. The hydrodynamic and Laplace pressures correspond to drop radius 50 μm approaching at 1 μm/s and interfacial tension 50 mN/m.

by eq 1; the time at which coalescence occurs is also predicted accurately. Although these salts are known to be chaotropic (KI) or kosmotropic ($NaClO_4$), they exhibited no detectable effect on the coalescence behavior. Videos illustrating the different types of coalescence events for PFX drops are provided as Movies 1 and 2.

In the upper pane of Figure 4C, we compare the range and magnitude of the disjoining pressure due to the exponential hydrophobic attraction with that for the vdW attraction in air−water−air and PFO−water−PFO planar systems. A comparison of DLVO, hydrophobic and hydrodynamic pressures, pertinent to understanding dynamic interactions between drops, is shown in the lower pane of Figure 4C. Drop deformation is expected to be a significant consideration when the magnitude of the total pressure becomes comparable to the Laplace pressure. This comparison illustrates how the range and intensity of different forces act in concert to determine the instability of drops when the aqueous film thins to between 2 and 4 nm.

By using pure, inert, and highly water-insoluble, hydrophobic oils and by suppressing effects due to electrostatics, van der Waals and capillary forces, we have isolated the hydrophobic attraction in a soft matter system. This attraction stems from water molecules acting to minimize disruption to their hydrogen bonding network at nonpolar surfaces. Its range and intensity is deduced by modulating this attraction with three different types of repulsive forces in drop coalescence experiments. As expected from its molecular origin, the characteristic decay length of 0.30 ± 0.03 nm is consistent with the molecular dimension of water and theoretical prediction,[22,23] giving rise to a very steep attraction compared to DLVO forces. It is remarkable that at the onset of coalescence, with critical film thickness ∼3 nm, the hydrophobic interaction energy per water molecule in the film is only $\sim 10^{-5}$ kT. Even if the same interaction energy is attributed to only the first layer of water molecules at the oil−water interface, the energy per molecule is just 5 times larger. This is 2 to 3 orders of magnitude smaller than the interfacial energy of the oil/water interface, which equates to ∼0.01 kT per water molecule at the interface. This may explain why this fundamental interaction has for so long evaded systematic detection.

Given the simplicity of the system we have used, the hydrophobic attraction observed here is expected to be universal in water-hating systems, from the molecular to the macroscopic. Therefore it will impact on a range of processes from self-assembled monolayer formation to protein folding kinetics to emulsion stability. It is clear that by accounting for this force, more accurate models and a greater understanding of the hydrophobic effect can be attained. Furthermore, through careful material choice, the interaction can be potentially exploited in nanoscale devices.

METHODS

Materials. Index matched PFX drops were made by mixing PFO and PFB underwater at a mass ratio of 54:46. PFO and PFB were obtained from Sigma-Aldrich and purified by repeated flash chromatography over activated magnesium silicate (Florisil, Sigma-Aldrich) until a stable value for the interfacial tension with water was obtained. Deionized water was from a Millipore Milli-Q Direct system, with a minimum resistivity of 18.4 MΩ cm. Substrates used in AFM measurements were 50 mm Petri dishes, boiled in absolute ethanol for 3 h to give a surface with a water contact angle in air of ∼30°.

Experimental Protocols. Oil droplets were generated underwater by discharging a glass syringe containing a few microlitres of oil in a few hundred microlitres of water. AFM cantilevers were fabricated from silicon wafers using nanolithography with dimensions ∼350 μm × 50 μm × 2 μm. Typical spring constants were 0.1−0.3 N/m as measured by the Hutter and Bechhoefer method.[27] A circular gold patch (radius 22 μm) was added at the free end of the cantilever, and hydrophobized by immersion in 1 mM decanethiol. A PFX droplet was attached to this hydrophobized patch by bringing the cantilever down manually over a suitably sized droplet on the substrate. This was then lifted up and moved over another drop in order to perform a measurement. Experiments were arranged and aligned using a Nikon TE2000 inverted microscope to ensure axisymmetry; the negligible effect of minor misalignment is shown in the Supporting Information. Phase contrast illumination was used to make the index-matched drops more visible. AFM measurements were made using an Asylum Research MFP-3D equipped with ARC1 controller, and independently on a JPK Nanowizard 3. The normal (z-axis) motion of the piezo drive was independently measured during experiments using a linear variable differential transformer (MFP3D) or capacitive sensor (NW3). Theoretical modeling of experimental results is based on the Stokes−Reynolds−Young−Laplace model that includes effects of drop deformation, hydrodynamic interaction and disjoining pressure between the interacting drops.[19]

ASSOCIATED CONTENT

Supporting Information

Extensive details of experimental, analysis, and modeling protocols. This material is available free of charge via the Internet at http://pubs.acs.org.

Web-Enhanced Features

Videos illustrating the different types of coalescence events for PFX drops are available as Movies 1 and 2 in the HTML version of this paper.

AUTHOR INFORMATION

Corresponding Authors

*E-mail: Rico.Tabor@monash.edu.au.
*E-mail: D.Chan@unimelb.edu.au.

Notes

The authors declare no competing financial interest.

ACKNOWLEDGMENTS

This research is supported in part by the Australian Research Council through a Discovery Project Grant. C.W. is supported by an Australian Postgraduate Research Award.

REFERENCES

(1) Perram, C. M.; Nicolau, C.; Perram, J. W. Interparticle Forces in Multiphase Colloid Systems: The Resurrection of Coagulated *Sauce Béarnaise*. *Nature* **1977**, *270*, 572−573.

(2) Dyson, H. J.; Wright, P. E.; Scheraga, H. A. The Role of Hydrophobic Interactions in Initiation and Propagation of Protein Folding. *Proc. Natl. Acad. Sci. U. S. A.* **2006**, *103*, 13057−13061.

(3) Israelachvili, J. N.; Pashley, R. M. The Hydrophobic Interaction is Long Range, Decaying Exponentially with Distance. *Nature* **1982**, *300*, 341−342.

(4) Meyer, E. E.; Rosenberg, K. J.; Israelachvili, J. N. Recent Progress in Understanding Hydrophobic Interactions. *Proc. Natl. Acad. Sci. U. S. A.* **2006**, *103*, 15739−15746.

(5) Christenson, H. K; Claesson, P. M. Direct Measurements of the Force Between Hydrophobic Surfaces in Water. *Adv. Colloid Interaface Sci.* **2001**, *91*, 391−436.

(6) Hammer, M. U.; Anderson, T. H.; Chaimovich, A.; Shell, M. S.; Israelachvili, J. N. The Search for the Hydrophobic Force Law. *Faraday Discuss.* **2010**, *146*, 299−308.

(7) Blake, T. D; Kitchener, J. A. Stability of Aqueous Films on Hydrophobic Methylated Silica. *J. Chem. Soc., Faraday Trans. 1* **1972**, *68*, 1435−1442.

(8) Israelachvili, J. N. *Intermolecular and Surface Forces*; Academic: New York, 1992.

(9) Zhang, X. Y.; Zhu, Y. X.; Granick, S. Softened Hydrophobic Attraction Between Macroscopic Surfaces in Relative Motion. *J. Am. Chem. Soc.* **2001**, *123*, 6736−6737.

(10) Miklavic, S. J; Chan, D. Y. C.; White, L. R.; Healy, T. W. Double-Layer Forces Between Heterogeneous Charged Surfaces. *J. Phys. Chem.* **1994**, *98*, 9022−9032.

(11) Donaldson, S. H., Jr; Lee, C. T.; Chmelka, B. F.; Israelachvili, J. N. General Hydrophobic Interaction Potential for Surfactant/Lipid Bilayers from Direct Force Measurements between Light Modulated Bilayers. *Proc. Natl. Acad. Sci. U. S. A.* **2011**, *108*, 15699−15704.

(12) Ishida, N.; Sakamoto, M.; Miyahara, M.; Higashitani, K. Attraction Between Hydrophobic Surfaces with and without Gas Phase. *Langmuir* **2000**, *16*, 5681−5687.

(13) Attard, P. Themodynamic Analysis of Bridging Bubbles and a Quantitative Comparison with the Measured Hydrophobic Attraction. *Langmuir* **2000**, *16*, 4455−4466.

(14) Christenson, H. K.; Claesson, P. M. Cavitation and the Interaction Between Macroscopic Hydrophobic Surfaces. *Science* **1988**, *239*, 390−392.

(15) Dagastine, R. R.; Manica, R.; Carnie, S. L.; Chan, D. Y. C.; Stevens, G. W.; Grieser, F. Dynamic Forces between Deformable Drops in Water. *Science* **2006**, *313*, 210−213.

(16) Vakarelski, I. U.; Manica, R.; Dagastine, R. R.; Tang, X.; O'Shea, S. J.; Stevens, G. W.; Grieser, F.; Chan, D. Y. C. Dynamic Interactions between Microbubbles in Water. *Proc. Natl. Acad. Sci. U. S. A.* **2010**, *107*, 11177−11182.

(17) Tabor, R. F.; Wu, C.; Lockie, H.; Manica, R.; Chan, D. Y. C.; Grieser, F.; Dagastine, R. R. Homo- and Hetero-Interactions between Air Bubbles and Oil Droplets Measured by Atomic Force Microscopy. *Soft Matter* **2011**, *7*, 8977−8983.

(18) Neeson, M.; Tabor, R. F.; Grieser, F.; Dagastine, R. R.; Chan, D. Y. C. Compound Sessile Drops. *Soft Matter* **2012**, *8*, 11042−11050.

(19) Tabor, R. F.; Grieser, F.; Dagastine, R. R.; Chan, D. Y. C. Measurement and Analysis of Forces in Bubble and Droplet Systems using AFM. *J. Colloid Interface Sci.* **2012**, *371*, 1−14.

(20) Chan, D. Y. C.; Klaseboer, E.; Manica, R. Theory of Non-Equilibrium Force Measurements Involving Deformable Drops and Bubbles. *Adv. Colloid Interface Sci.* **2011**, *165*, 70−90.

(21) Carnie, S. L.; Chan, D. Y. C.; Lewis, C.; Manica, R.; Dagastine, R. R. Measurement of Dynamical Forces between Deformable Drops Using the Atomic Force Microscope. I. Theory. *Langmuir* **2005**, *21*, 2912−2922.

(22) Lum, K.; Chandler, D.; Weeks, J. D. Hydrophobicity at Small and Large Length Scales. *J. Phys. Chem. B* **1999**, *103*, 4570−4577.

(23) Huang, D. M.; Chandler, D. The Hydrophobic Effect and the Influence of Solute−Solvent Attractions. *J. Phys. Chem. B* **2002**, *106*, 2047−2053.

(24) Bremond, N.; Thiam, A. R.; Bibette, J. Decompressing Emulsion Droplets Favours Coalescence. *Phys. Rev. Lett.* **2008**, *100*, 024501.

(25) Tabor, R. F.; Manica, R.; Chan, D. Y. C.; Grieser, F.; Dagastine, R. R. Repulsive van der Waals Forces in Soft Matter: Why Bubbles Do Not Stick to Walls. *Phys. Rev. Lett.* **2011**, *106*, 64501.

(26) Argyris, D.; Phan, A.; Striolo, A.; Ashby, P. D. Hydration Structure at the α-Al_2O_3 (001) Surface: Insights from Experimental Atomic Force Spectroscopic Data and Atomistic Molecular Dynamics Simulation. *J. Phys. Chem. C* **2013**, *117*, 10433−10444.

(27) Hutter, J. L.; Bechhoefer, J. Calibration of Atomic-Force Microscope Tips. *Rev. Sci. Instrum.* **1993**, *64*, 1868−1873.